The following article appeared in Physics of Fluids 34, 026603 (2022) and may be found at https://doi.org/10.1063/5.0078474.

Dispersion of a Fluid Plume During Radial Injection in an Aquifer

Benjamin W.A. Hyatt[1] and Yuri Leonenko[1, a)]
Department of Earth and Environmental Sciences, University of Waterloo, Waterloo, Ontario N2L 3G1, Canada

(*Electronic mail: leonenko@uwaterloo.ca.)

(Dated: 29 December 2021)

This study outlines a model for radial injected fluid flow with mechanical dispersion in a vertically confined porous aquifer. Existing studies have investigated fully segregated fluid flow in this setting, where the injected fluid and resident fluid form a propagating sharp interface. The present study uses the geometry of these sharp interfaces as a basis for the velocity field to take into account dispersion and buoyancy/viscosity effects. By differentiating the radial position of the sharp interface with respect to time, a time dependent radial velocity field governing the flow is obtained. Evaluating this radial velocity at the moment the original interface were to intersect a given position gives a velocity field which is a function of the position coordinates inside the aquifer. Using this velocity field, the fluids saturation profile resulting from mechanical dispersion can be found analytically. It is shown that the concentration of the injected fluid smoothly decays around the position of the corresponding sharp interface, allowing for the injected fluid to be present in detectable quantities beyond the extent of these solutions. This concentration spread should be considered in defining outer boundaries on fluids in injection well projects such as carbon sequestration or groundwater applications.

I. INTRODUCTION

The flow of fluids injected into porous aquifers has been a research area of interest for decades, having wide ranging applications including enhanced oil recovery[1–3], assessing drinking water quality[4] and carbon capture and storage (CCS)[5,6]. This has inspired the development of many analytical solutions and numerical simulations modelling the behaviour, geometry and evolution of fluids being injected into the resident brine of aquifers under a variety of circumstances. A common feature throughout many of these studies is the assumption that the injected fluid and resident fluid experience no dispersion or miscibility; that is, the injected fluid and the resident fluid form a "sharp interface" separating regions of 100% injected fluid saturation and 100% brine saturation[7–10]. Another assumption that allows for simple, approximate solutions for the fluids' evolution in the aquifer is vertical equilibrium, where the flow velocity in the vertical direction is assumed to be negligible and the velocity field in the aquifer is strictly radial and directed outward from the injection site[11–13].

With simplifying assumptions and boundary conditions, analytical solutions for the time evolution and shape of this sharp interface (due to effects such as buoyancy) as a function of radial distance from the injection well and time can be obtained. Thus, the furthest radial extent of the injected fluid can be determined after a certain period of time. However, traces of the injected fluid may appear beyond the sharp interface's extent due to mechanical dispersion, a mass transfer mechanism where velocity changes on the scale of the medium's pores cause the fluid to spread out[14]. This will cause the saturation of the injected fluid (or, the "concentration" of an injected solute) to smoothly decay around the region where the sharp interface would otherwise be. This phenomenon has been examined in studies that assume a radial flow of injected fluid with no vertical dependence or buoyancy effects[15,16].

This strictly radial flow with mechanical dispersion can be mathematically interpreted as having a velocity field governed by an *underlying* cylindrical, ficticious sharp interface, which itself is a special vertically-independent case of a general 2-D sharp interface. The flow that is being considered presently is *not* for the fully segregated fluids case; instead, the geometry of a general sharp interface that arises due to buoyancy and viscosity effects is used to determine the geometry of the smooth saturation profile which arises due to mechanical dispersion. In the limit of the dispersivity diminishing to zero, the concentration profile converges to the sharp interface, with distinguishable, saturated concentration regions on either side. A nonzero dispersivity results in a saturation gradient near the would-be position of a sharp interface.

The present study proposes a mathematical procedure for obtaining the position dependent velocity field and saturation profile of fluids in a vertically confined porous aquifer with mechanical dispersion, using a corresponding sharp interface function. With a radially directed but vertically dependent velocity field thus obtained, a 1-D, vertically independent concentration solution can be extended to a 2-D profile. In recent years, a number of analytical and computational studies have endeavored to formulate 2-D concentration profile solutions[17–21]. However, the vertical dependence of the concentration typically considered is due to diffusion/dispersion alone. Instead, by extending sharp interface solutions (which are produced with gravity/buoyancy already considered) to the miscible/non-zero dispersion case to obtain the concentration solution, the presently proposed technique incorporates the effects of gravity in the solution and its impact on the evolution of the concentration profile.

This allows for quantifying an upper boundary cutoff for the distances at which traces of the injected fluid may appear in the aquifer: for example, finding where the relative concentration of the injected fluid drops to some acceptable levels,

a)Also at Department of Geography and Environmental Management, University of Waterloo, Waterloo, Ontario N2L 3G1, Canada

TABLE I. A nomenclature table for symbols and terms used throughout the present analysis

Symbol/Variable	Quantity	SI Units
$A(z)$	Denotes a family of functions which can characterize the fluids' flow velocity	$m^2 s^{-1}$
α	A constant equal to $(2/\sqrt{3})\text{erfc}^{-1}\{0.02\}$, defined for brevity	None
c	Concentration of species injected into the aquifer	mol m^{-3}
c_o	Initial concentration of injected fluid when entering aquifer	mol m^{-3}
d	Dispersivity length (no subscript denotes radial scale)	m
D_m	Coefficient of molecular diffusion	$m^2 s^{-1}$
$d\boldsymbol{\Sigma}$	Differential vector area	m^2
$\Delta\rho$	Density difference between fluids (taken to be positive)	kg m^{-3}
$f(M,\Gamma)$	Dimensionless function of M and Γ, defined for brevity	None
g	Acceleration due to gravity	m s^{-2}
Γ	Dimensionless parameter related to bouyancy effects	None
h	Height of the sharp interface formed between immiscible fluids (function of r and t)	m
H	Overall height of the aquifer (constant)	m
θ	Angular cylindrical coordinate	None
k	Permeability of the aquifer	m^2
M	Ratio of the resident and injected fluids' viscosities	None
μ	Viscosity (subscripts r and i denote resident and injected fluids respectively)	kg $m^{-1} s^{-1}$
Q	Volumetric injection rate (assumed constant)	m^3 s^{-1}
$\boldsymbol{q}$	Darcy velocity from Darcy's law (equal to the flow velocity scaled by the porosity)	m s^{-1}
r	Radial cylindrical coordinate (normal to injection well located at $r = 0$)	m
r_1	Radial position (at $z = 0$ m) of the aquifer region where $c/c_o = 0.01$	m
r_2	Radial position (at $z = 0$ m) of sharp interface solution	m
R_1, R_2	Dimensionless forms of r_1, r_2 above (normalized by d)	None
t	Time	s
T	Dimensionless time variable	None
T_{crit}	Dimensionless time after which the function $R_1(T) - R_2(T)$ increases monotonically	None
$\boldsymbol{v}$	Flow velocity (vector when bolded, scalar magnitude when unbolded)	m s^{-1}
W_0	Lambert W Function	None
ϕ	Porosity	None
z	Vertical cylindrical coordinate (positive downward, $z = 0$ m is at the top of the aquifer, injection well coincides with axis)	m

such as 1%, 0.5%, etc. Similarly, a lower boundary distance value for a desired relative concentration cutoff (e.g., 99%) can be defined to quantify regions in the aquifer that are effectively saturated with the injected fluid. The presence of injected fluids is of great interest in injection well engineering applications[22–25]. As such, computing these concentration boundaries between regions saturated with residual fluid, injection fluid, or an intermediate transition zone will be of practical in determining injection efficiency and safety parameters.

For the purposes of this investigation, the resident and injected fluids are assumed to have velocity fields which obey Darcy's law and are incompressible with constant densities and viscosities. The vertical pressure throughout the aquifer is assumed to be hydrostatic, and the aquifer is assumed to be isothermal, with a finite height due to impermeable caprock layers at the top and bottom and an infinite lateral extent. Furthermore, the aquifer is assumed to have constant permeability, porosity, and dispersivity scale.

II. METHODOLOGY

The mathematical expression for the incompressibility condition of a fluid states that the divergence of its velocity field is zero[26]:

$$\nabla \cdot \boldsymbol{v} = 0 \tag{1}$$

Assuming an axisymmetric flow with vertical equilibrium, the velocity field in cylindrical coordinates will only have a component in the radial direction, outward from the injection well; this radial velocity assumption is applied by Guo et al.[27], whose sharp interface solutions are considered in section III. To satisfy the incompressibility condition, this radial velocity field must be of the form:

$$\boldsymbol{v} \propto \frac{1}{r}\hat{\boldsymbol{r}} \tag{2}$$

Where $\hat{\boldsymbol{r}}$ is the radial unit vector directed normally outward from the injection site. In the case where the injected and resident fluids do not experience disperision, a sharp interface

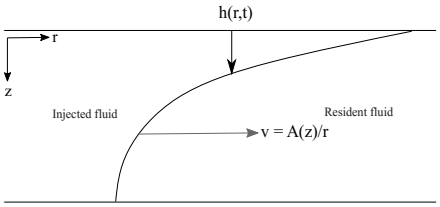

FIG. 1. A travelling sharp interface in a vertically confined aquifer

between the two radiates through the aquifer during injection. Due to density and viscosity differences between the fluids, the interface may take on a curved shape where the injected and resident fluids are vertically segregated. These interfaces can be expressed by a height function h (m) that depends on the radial distance r (m) from the aquifer and the time elapsed during injection, t (s). Figure 1 depicts the motion of an arbitrarily shaped interface travelling with radial velocity of the incompressible form $v = A(z)/r$ (m s^{-1}), where $A(z)$ (m^2 s^{-1}) is a scalar function which accounts for effects such as buoyancy.

The continuity equation for the injected fluid interface is given by:

$$\phi \frac{\partial h}{\partial t} + \nabla \cdot (h\boldsymbol{q}) = 0 \tag{3}$$

Where $\boldsymbol{q}$ is the Darcy velocity from Darcy's law (m s^{-1}) and ϕ is the aquifer's porosity, which is the fraction of volume in the medium that is open and unoccupied of material (dimensionless). Equation 3 can be expressed in terms of the flow velocity $\boldsymbol{v}$ by scaling the equation by the factor $\frac{1}{\phi}$. Thus,

$$\frac{\partial h}{\partial t} + \nabla \cdot (h\boldsymbol{v}) = 0 \tag{4}$$

Which in a cylindrical coordinate system with a strictly radial $\boldsymbol{v}$ field can be written:

$$\frac{\partial h}{\partial t} + \frac{1}{r}\frac{\partial}{\partial r}(rhv) = 0 \tag{5}$$

The resident and injected fluids are both assumed to have hydrostatic fluid pressure and velocity fields governed by Darcy's law (i.e. proportional to the pressure gradient of each fluid). The mathematical expressions for these assumptions can be combined with equation 5 to obtain the governing differential equation for the interface's evolution:

$$\frac{\partial h}{\partial t} - \frac{1}{r\phi}\left(\frac{g\Delta\rho kh(H-h)r}{\mu_r h + \mu_i(H-h)}\frac{\partial h}{\partial r} + \frac{Q\mu_i(H-h)}{2\pi(\mu_r h + \mu_i(H-h))}\right) = 0 \tag{6}$$

Here, Q is assumed to be a constant volumetric injection rate at the site of the well (m^3 s^{-1}); the μ_r and μ_i terms are the viscosities of the residual and injected fluids respectively (kg m^{-1} s^{-1}), $\Delta\rho$ is their density difference (kg m^{-3}), H is the height of the aquifer (m), k is its permeability (m^2), and g is the acceleration due to gravity (m s^2). This form of the equation appears in studies by Nordbotten and Celia[12] as well as Guo et al.[27], who derive approximate solutions for it given various fluid properties.

Given an interface solution to equation 6 of the form $h(r,t)$, a position dependent velocity field which guides the fluids can be obtained as follows: rearrange the equation 6 solution for the radial distance of the interface $r(z,t)$, where the interface height value h has been rebranded as the generic vertical position coordinate z since the current procedure seeks a position dependent function, defined throughout the entire aquifer domain. The partial derivative $\partial r/\partial t$ will give the radial velocity (assumed to be the only component) as a function of z and t. The original equation 6 solution can be rearranged once more, solving for time. The function $t(r,z)$ gives the time at which a certain point (r,z) inside the aquifer is intersected by the travelling interface. This time is used to evaluate the radial velocity given by $\partial r/\partial t$, as the fluids' velocity field at a certain position is expected to be given by the would-be speed of the travelling interface solution as it intersects that position. Substituting $t(r,z)$ into the $\partial r/\partial t$ function will give the radial velocity as a function of position.

It is assumed that the velocity field that guides the sharp interface also globally guides the fluids in the aquifer, since fluid continues to flow "behind" the location of the interface and "beyond" it as the resident fluid is displaced. This assumption is expected to hold at least locally near the would-be position of the sharp interface where property differences between the injected and resident fluids prominently effect their flow. In the presence of mechanical dispersion, this gives rise to an injectant concentration profile which is smoothly "spread" around the position of the corresponding interface solution, as expected when mechanical dispersion is included. Far away from this location are regions of nearly saturated concentrations (close to 100% and 0%).

Consider the simplest case of the z-independent, cylindrical sharp interface where the effects of gravity are neglected. The volume injected over time can be expressed as:

$$Qt = \pi r^2 H\phi \tag{7}$$

Which gives radial distance and time functions:

$$r(t) = \sqrt{\frac{Qt}{\pi H\phi}} \tag{8}$$

$$t(r) = \frac{\pi r^2 H\phi}{Q} \tag{9}$$

Taking the derivative with equation 8 respect to time (a total derivative in this special z-independent case):

$$\frac{dr}{dt} = \frac{1}{2}\sqrt{\frac{Q}{\pi H\phi t}} \tag{10}$$

Substituting in the "intersection time" given in equation 9 gives:

$$\frac{dr}{dt} = v(r) = \frac{Q}{2\pi H \phi r} \tag{11}$$

Which is consistent with the incompressibility condition seen in equation 2 and the velocity expression used in studies of radial flow in aquifers with mechanical dispersion such as Tang and Babu[16]. In general, applying this procedure to an interface solution of equation 6 will yield an incompressible velocity field of the form:

$$\boldsymbol{v} = \frac{A(z)}{r}\hat{\boldsymbol{r}} \tag{12}$$

Where the term $A(z)$ is a function of z characteristic of the analytical interface solution's properties such as buoyancy. In the case of the cylindrical interface, A is a constant equal to $Q/2\pi\phi H$, which is independent of gravity/density as expected.

An expression for the velocity field must also be consistent with the volumetric injection rate of the fluid Q evaluated through some effective surface (elaborated on below), which is given by the total volumetric flux through that surface[26]:

$$Q = \phi \iint \boldsymbol{v} \cdot d\boldsymbol{\Sigma} \tag{13}$$

The porosity factor is introduced to relate the actual flow velocity with the volumetric flux from Darcy's law[28]. For the purposes of this investigation, the porosity is assumed to be constant throughout the aquifer. If the surface used to evaluate the flux integral in equation 13 is a cylinder and the velocity field is assumed to be strictly radial, the area element dotted with it can be written as:

$$\boldsymbol{v} \cdot d\boldsymbol{\Sigma} = v(rd\theta dz) \tag{14}$$

Where θ is the dimensionless azimuthal angle coordinate (all fields in this study are considered independent of θ). The flux integral on the right-hand side of equation 13 can be trivally evaluated with the cylindrical velocity field from equation 11.

In reality, the interface between injected and residual fluids is never sharp. There is always dispersion of the fluids due to mass transfer effects taking place at the interface. Such processes are governed by the advection-diffusion equation (ADE), which has the general form[29]:

$$\frac{\partial c}{\partial t} = \nabla \cdot (\boldsymbol{D}\nabla c) - \nabla \cdot (\boldsymbol{v}c) + P \tag{15}$$

Here, c is the concentration of a solute (mol m^{-3}) which in the present case comes along with the injected fluid, $\boldsymbol{D}$ is the diffusivity (a tensor, in general[30]) (m^2 s^{-1}) and P represents sources and sinks (mol m^{-3} s^{-1}). In the domain of the aquifer outside of the injection site, it is assumed that $P = 0$. The diffusivity term is taken to be the sum of the molecular diffusion and mechanical dispersion effects (e.g. as done by Neuman et al.[31]):

$$D_T = D_m + d_T\|\boldsymbol{v}\|, \quad D_L = D_m + d_L\|\boldsymbol{v}\| \tag{16}$$

Here, D_m is the molecular diffusion coefficient (m^2 s^{-1}), which is assumed constant, D_T and D_L are the transverse (normal to the velocity field) and longitudinal (parallel to the velocity field) diffusivity components respectively, and d_T and d_L are the transverse and longitudinal dispersivity scales (m). In the present study's case of a strictly radial velocity field in an isotropic medium, the transverse dispersivity is taken to be 0, and the longitudinal dispersivity d_L is simply referred to as the dispersivty d. It has been suggested that in large field scale transport situations, longitudinal dispersivity approaches a constant or asymptotic value at larger distances[32]. The asymptotic value (which is constant) can serve as a worst case scenario for evaluation of dispersion.

For many practical cases with a constant injection rate (and thus constantly present advection effects) and large injection scales considered, the effects of molecular diffusion can be assumed to be far less than those of mechanical dispersion; the magnitudes of these mass transfer effects behind this simplification are quantified in the CCS example given in section III D. With this assumption, the ADE can be simplified as:

$$\frac{\partial c}{\partial t} + \frac{A(z)}{r}\left(\frac{\partial c}{\partial r} - d\frac{\partial^2 c}{\partial^2 r}\right) = 0 \tag{17}$$

This form of the ADE and its solutions have been the subject of numerous hydrology studies. One of multiple approximate solutions in the literature given by Dagan[33] and Hsieh[34] is of practical interest as it has a tendency to slightly exceed numerical solutions to equation 17, thus acting as an "upper bound" estimate on the concentration profile in the aquifer. This concentration solution has the dimensional form:

$$c = \frac{c_o}{2}\mathrm{erfc}\left\{\frac{\left(\ln\left(\frac{r}{d}\right) - \ln\left(\frac{1}{d}\sqrt{2A(z)t + r_o^2}\right)\right)\left(2A(z)t + r_o^2\right)}{d^2\sqrt{\frac{4}{3d^3}\left(\left(2A(z)t + r_o^2\right)^{\frac{3}{2}} - r_o^3\right)}}\right\} \tag{18}$$

Solutions of the radial ADE given in equation 17 have continued to be developed in more recent studies, e.g. the power series concentration solution given by Lai et al.[35]. Other recent works, such as those by Hsieh and Yeh[36] and Huang et al.[37] consider two-zone concentration solutions. However, the present study makes use of many algebraic manipulations of the concentration solution (see section III), and does not consider a two-zone profile. For these reasons, as well as it remaining in good agreement with modern solutions and having aquifer/injection conditions comparable to the sharp interface studies such as e.g. Guo et al.[27] (considered in section III),

the concentration solution in equation 18 remains applicable for the puroses of demonstrating the proposed method.

In equation 18, r_o is the radius of the injection well (m), c_o is the initial concentration of the injected fluid (mol m^{-3}), and $A(z)$ is the term from the incompressible velocity field. For an aquifer of infinite radial extent, the injection well radius r_o can be neglected, giving the so called "line solution" as done by Guo et al.[27]. The above equation can also be solved for r as a function of time and concentration, which is of practical interest and allows for comparing the "cut off" for the extent of injected fluid presence with a sharp interface. After finding the velocity field for general interface geometries, the $A(z)$ term can be substituted into this equation to allow for z dependent solutions: this procedure is carried out in section III for some analytical sharp interface solutions.

Consider the form of the ADE in equation 17 in the limit of the dispersivity d going to 0 m:

$$\frac{\partial c}{\partial t}+\frac{A(z)}{r}\frac{\partial c}{\partial r}=0 \tag{19}$$

The solution to this modified ADE is:

$$c(r,z,t)=c_o u(\sqrt{2A(Z)t}-r), \quad t,r>0 \tag{20}$$

Where u denotes the Heaviside "step" function. In general, the ADE is applicable for fluids/solutes that are miscible. The result above for the limiting $d=0$ m case shows that the concentration profile of the injected and resident fluids becomes completely saturated on either side of a "sharp" boundary located at the variable distance $r=\sqrt{2A(z)t}$, even if the fluids are assumed to be miscible. This saturated profile is also the behaviour of a system with immiscible fluids which form a sharp interface between their saturated regions. Thus, the case of immiscible injected and resident fluids behaves the same as the case of miscible fluids with $d=0$ m, and sharp interface solutions for the former system can be used to obtain concentration profiles for the latter by "including" dispersion using the procedure outlined above.

III. RESULTS

To demonstrate this transformation, three injection driven sharp interface solutions for h as a function of r,t from Guo et al.[27] have been chosen for its application. For all these solutions, the injected fluid is assumed to be less dense than the resident fluid, while the driving effects of buoyancy are assumed to be far less than those of injection, with viscosity differences between the injected and resident fluids being the key factor in each solution's geometry. All three solutions are fixed to be $h=0$ and $h=H$ outside of two moving boundaries characteristic of each solution.

A. Injected Fluid is More Viscous than Resident Fluid

Under these circumstances, Guo et al.[27] provides the following "travelling interface" height solution:

$$h(r,t)=\frac{H(M-1)}{2M\Gamma}\left(\frac{\pi\phi Hr^2}{Qt}-1\right)+\frac{H}{2},$$
$$1-\frac{M}{1-M}\Gamma<\frac{\pi\phi Hr^2}{Qt}\leq 1+\frac{M}{1-M}\Gamma \tag{21}$$

Here, the dimensionless parameters $\Gamma=2\pi\Delta\rho gkH^2/\mu_r Q$ represents the effect of buoyancy compared to injection and $M=\mu_r/\mu_i$ is the ratio of the resident and injected fluids' viscosities. Mathematically, the solution in 21 assumes that $M<1$ and that $\Gamma\ll 1$, the latter being consistent with the vertical equilibrium/strictly radial velocity assumption.

Solving equation 21 for r as a function of t and z (where the latter is used to denote vertical variable instead of h as discussed in section II) yields:

$$r(z,t)=\sqrt{\frac{Qt}{\pi\phi H}\left(\frac{M\Gamma}{M-1}\left(\frac{2z}{H}-1\right)+1\right)} \tag{22}$$

And solving for the "intersection" time $t(r,z)$ yields:

$$t(r,z)=\frac{\pi\phi Hr^2}{Q\left(1+\frac{M\Gamma}{M-1}\left(\frac{2z}{H}-1\right)\right)} \tag{23}$$

Differentiating the radial position in equation 22 with respect to t yields:

$$\frac{\partial r}{\partial t}=\frac{1}{2}\sqrt{\frac{Q}{\pi\phi Ht}\left(\frac{M\Gamma}{M-1}\left(\frac{2z}{H}-1\right)+1\right)} \tag{24}$$

Substituting the intersection time from equation 23 into the derivative in equation 24 gives the radial velocity:

$$\frac{\partial r}{\partial t}=v(r,z)=\frac{Q\left(\frac{M\Gamma}{M-1}\left(\frac{2z}{H}-1\right)+1\right)}{2\pi\phi Hr} \tag{25}$$

Which is of the required incompressible form seen in equation 12:

$$\boldsymbol{v}=\frac{A(z)}{r}\hat{\boldsymbol{r}}, \quad A(z)=\frac{Q\left(\frac{M\Gamma}{M-1}\left(\frac{2z}{H}-1\right)+1\right)}{2\pi\phi H} \tag{26}$$

Note that as the buoyancy parameter Γ approaches 0, the velocity field above in equations 25 and 26 approaches that of the "cylindrical" case derived in equation 11. This is consistent with previously mentioned dispersion studies such as Tang and Babu[16] whose solutions assume no gravitational effects/vertical dependence for the fluids' profile. Furthermore, this velocity field is also consistent with the volume flux relation in equation 13; consider evaluating the surface integral from equation 13 through a cylindrical surface of radius $R>r_o$ centred at the injection site, such that the dot product element

can be written as in equation 14. Evaluating this integral with the velocity field in equation 25 yields:

$$\phi \int_0^H \int_0^{2\pi} \frac{Q\left(\frac{M\Gamma}{M-1}\left(\frac{2z}{H}-1\right)+1\right)}{2\pi\phi HR}(Rd\theta dz) = Q \qquad (27)$$

As required by the volume flux relation in equation 13. Using this velocity field, the 2-D concentration profile can be given by substituting $A(z)$ from equation 26 into equation 18 from Dagan[33]. Similarly, one can also rearrange this concentration equation for r, and find the radial extent of "boundaries" for which a specific concentration is present. Note that the concentration "boundaries" referred to hereafter are simply a sets of points in the concentration profile of a particular concentration. Two boundaries of practical interest are where $c/c_o = 0.99$, and $c/c_o = 0.01$, as these provide an approximation for a "transition zone" where the relative concentration of the injected fluid experiences the most variation due to dispersion; outside of these boundaries, the aquifer is essentially saturated with the resident or the injected fluid. The inverted concentration equation (including the line solution approximation $r_o \approx 0$) has the form:

$$r(c,z,t) = \sqrt{2A(z)t}\exp\left\{\frac{2}{(2A(z)t)^{\frac{1}{4}}}\sqrt{\frac{d}{3}}\text{erfc}^{-1}\left\{\frac{2c}{c_o}\right\}\right\} \qquad (28)$$

To demonstrate the practical importance of including mechanical dispersion, consider the radial extent of the $c/c_o = 0.01$ boundary at the top of the aquifer (at $z = 0$ for a positive-downward z-axis) where the immiscible interface solution in 21 is at its furthest radial extent; let these two radial extents be denoted r_1 and r_2 respectively. For clarity, let the function $f(M,\Gamma)$ be given as:

$$f(M,\Gamma) = \frac{M\Gamma}{1-M} + 1 \qquad (29)$$

Evaulating $A(z)$ from equation 26 at $z = 0$ gives:

$$A(0) = \frac{Q}{2\pi\phi H} f(M,\Gamma) \qquad (30)$$

Additionally, let the parameter α be given by:

$$\alpha = \frac{2}{\sqrt{3}}\text{erfc}^{-1}\{0.02\} \qquad (31)$$

Using the $A(0)$, α and $f(M,\Gamma)$ terms above and $c/c_o = 0.01$ in equation 28 gives the r_1 term:

$$r_1(t) = \sqrt{\frac{Qt}{\pi\phi H} f(M,\Gamma)}\exp\left\{\alpha\sqrt{d}\left(\frac{Qt}{\pi\phi H} f(M,\Gamma)\right)^{\frac{-1}{4}}\right\} \qquad (32)$$

Furthermore, let the dimensionless parameters for time and radial distance be T and R respectively, defined as:

$$T = \frac{Qt}{d^2\pi\phi H}, \qquad R = \frac{r}{d} \qquad (33)$$

Using these parameters, equation 32 can be nondimensionalized as:

$$R_1(T) = \sqrt{f(M,\Gamma)T}\exp\left\{\alpha\left(f(M,\Gamma)T\right)^{\frac{-1}{4}}\right\} \qquad (34)$$

The term r_2 can be found by evaluating equation 22 at $z = 0$:

$$r_2(t) = \sqrt{\frac{Qt}{\pi\phi H} f(M,\Gamma)} \qquad (35)$$

Note that as the disersivity length $d \to 0^+$, the radial extent of the 1% relative concentration boundary $r_1(t)$ in equation 32 converges to the radial extent of the sharp interface $r_2(t)$ in equation 35. This is consistent with the concentration profile becoming saturated on either side of the sharp interface solution in the absence of mechanical dispersion, as expected due to the Guo *et al.*[27] solutions being derived under the assumption of no dispersion. The expression for $r_2(t)$ can be nondimensionalized with the T and R parameters:

$$R_2(T) = \sqrt{f(M,\Gamma)T} \qquad (36)$$

Finally, the dimensionless difference between the 1% concentration boundary and the $M < 1$ sharp interface solution positions at $z = 0$ can be written as:

$$R_1(T) - R_2(T) = \sqrt{f(M,\Gamma)T}\left(\exp\left\{\alpha\left(f(M,\Gamma)T\right)^{\frac{-1}{4}}\right\} - 1\right) \qquad (37)$$

Note that the function $R_1(T) - R_2(T)$ in equation 37 is strictly positive for $T > 0$ and $0 < M < 1$. This is consistent with the concentration profile of the injected fluid being "spread" (due to mechanical dispersion) around the location of the sharp interface solution, with traces of the injected fluid appearing beyond the furthest radial extent of the sharp interface. The plot in figure 2 shows this dimensionless separation $R_1(T) - R_2(T)$ between the 1% boundary and the immiscible interface for $\Gamma = 0.05$ and $T = 10, 100$ and 1000.

While the dimensionless separation function is always positive, its time derivative with respect to T is initially negative; in other words, the position of the $c/c_o = 0.01$ concentration boundary initially gets closer to the position of the corresponding sharp interface solution, but then recedes from it indefinitely. This increased separation after an early critical time is illustrated in figure 2. The seperation's derivative function is given by:

$$\frac{\partial(R_1 - R_2)}{\partial T} = \frac{1}{2}\sqrt{\frac{f(M,\Gamma)}{T}}\left(\exp\left\{\alpha\left(f(M,\Gamma)T\right)^{\frac{-1}{4}}\right\} - 1\right) - \frac{\alpha}{4}\left(\frac{f(M,\Gamma)}{T^3}\right)^{\frac{1}{4}}\exp\left\{\alpha\left(f(M,\Gamma)T\right)^{\frac{-1}{4}}\right\} \qquad (38)$$

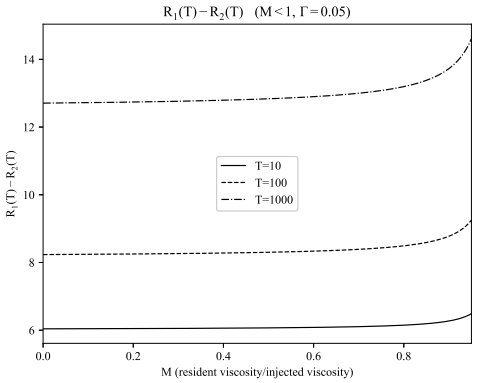

FIG. 2. The dimensionless difference between the 1% relative concentration boundary and the immiscible interface solution at the top of the aquifer ($M < 1$)

The critical dimensionless time T_{crit} after which $R_1(T) - R_2(T)$ increases monotonically with time (the root of equation 38) can be expressed in terms of the Lambert W function:

$$T_{crit} = \frac{1}{f(M,\Gamma)}\left(\frac{\alpha}{W_0\{-2e^{-2}\}+2}\right)^4 \tag{39}$$

E.g for $M = 0.5$ and $\Gamma = 0.05$, the separation $R_1(T) - R_2(T)$ increases monotonically with time after $T \approx 1.9$. This monotonic increase in the seperation function highlights the importance in considering mechanical dispersion in injection wells: over time, traces of the injected fluid appear increasingly beyond their location given by a sharp interface solution.

B. Injected Fluid is Less Viscous than Resident Fluid

The approximate solution provided by Guo et al.[27] for a more viscous resident fluid ($M > 1$) is:

$$h(r,t) = \frac{H}{M-1}\left(\sqrt{\frac{QMt}{\pi\phi H r^2}} - 1\right), \qquad \frac{Q}{\pi\phi HM} < \frac{r^2}{t} \leq \frac{QM}{\pi\phi H} \tag{40}$$

As before, rearranging this sharp interface height solution for its radial distance (as a function of t and z) and for the time t the sharp interface intersects a position (r,z) gives:

$$r(z,t) = \frac{1}{\left(\frac{z(M-1)}{H}+1\right)}\sqrt{\frac{QMt}{\pi\phi H}} \tag{41}$$

$$t(r,z) = \frac{\pi\phi H r^2}{QM}\left(\frac{z(M-1)}{H}+1\right)^2 \tag{42}$$

Differentiating the radial position in equation 41 with respect to time and substituting in the "intersection" time from equation 42 gives the radial velocity expression for this case:

$$\boldsymbol{v} = \frac{A(z)}{r}\hat{\boldsymbol{r}}, \quad A(z) = \frac{QM}{2\pi\phi H\left(\frac{z(M-1)}{H}+1\right)^2} \tag{43}$$

The original sharp interface solution given by Guo et al.[27] was derived without the buoyancy term Γ. However, in the limit that the viscosity ratio $M \to 1^+$, the velocity field in equation 43 reduces to the cylindrical, z-independent case, similarly to the velocity field in equation 26. This velocity field for the $M > 1$ case is also consistent with the volumetric flux integral from equation 13, and evaluating the surface integral through a cylindrical surface (as in equation 27 yields the required relation:

$$\phi\int_0^H\int_0^{2\pi}\frac{QM}{2\pi\phi H\left(\frac{z(M-1)}{H}+1\right)^2 R}(Rd\theta dz) = Q \tag{44}$$

Once again, consider the radial extents (at the top of the aquifer) of the 1% relative concentration boundary (r_1) and the immiscible solution (r_2) for the $M > 1$ case. Evaluating equation 28 at $z = 0$ with $A(z)$ from equation 43 gives the following expression for r_1:

$$r_1(t) = \sqrt{\frac{QMt}{\pi\phi H}}\exp\left\{\alpha\sqrt{d}\left(\frac{QMt}{\pi\phi H}\right)^{\frac{-1}{4}}\right\} \tag{45}$$

Where the same α constant defined in equation 31 is used. The furthest radial extent of the sharp interface solution is obtained by evaluating equation 41 at $z = 0$:

$$r_2(t) = \sqrt{\frac{QMt}{\pi\phi H}} \tag{46}$$

Once again, taking the limit of $d \to 0^+$ of $r_1(t)$ yields $r_2(t)$, recovering the sharp interface dividing a saturated "concentration" profile between the fluids when mechanical dispersion is excluded. Nondimensionalizing these terms with the same parameters T and R as defined above gives the dimensionless separation for the 1% boundary and the immiscible solution at $z = 0$ for the $M > 1$ case:

$$R_1(T) - R_2(T) = \sqrt{MT}\left(\exp\left\{\alpha\,(MT)^{\frac{-1}{4}}\right\} - 1\right) \tag{47}$$

This dimensionless seperation of the 1% concentration boundary and the original sharp interface at the top of the aquifer is once more a strictly positive function for $T > 0$ and $M > 1$, demonstrating that traces of the injected fluid will extend further than the sharp interface position when mechanical dispersion is included. As in the $M < 1$ case, differentiating

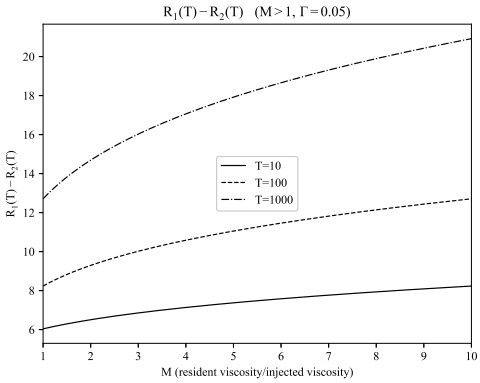

FIG. 3. The dimensionless difference between the 1% relative concentration boundary and the immiscible interface solution at the top of the aquifer ($M > 1$)

the seperation function above shows that the seperation initially decreases before increasing monotonically after a critical T_{crit}, which has an expression of the same form as equation 48 (as equation 47 of the same form as equation 37):

$$T_{crit} = \frac{1}{M}\left(\frac{\alpha}{W_0\{-2e^{-2}\}+2}\right)^4 \tag{48}$$

E.g. for $M = 5$, $T_{crit} \approx 0.4$. A plot of $R_1(T) - R_2(T)$ for the $M > 1$ case is shown in figure 3 for $T = 10, 100$ and 1000 for $1 < M < 10$.

C. Equal Viscosity for Injected Fluid and Resident Fluid

The sharp interface solution provided by Guo et al.[27] for fluids of equal viscosity ($M = 1$) is:

$$h(r,t) = \frac{H}{2}\left(1 - \frac{1}{\sqrt{\Gamma}}\left(\frac{\pi\phi H r^2}{Qt} - 1\right)\right), \quad \frac{Q}{\pi\phi H}(1-\sqrt{\Gamma}) < \frac{r^2}{t} \leq \frac{Q}{\pi\phi H}(1+\sqrt{\Gamma}) \tag{49}$$

Inverting this function and repeating the same procedure as done in the $M < 1$ and $M > 1$ cases gives the yields the following velocity field:

$$\boldsymbol{v} = \frac{A(z)}{r}\hat{\boldsymbol{r}}, \quad A(z) = \frac{Q}{2\pi\phi H}\left(1 - \sqrt{\Gamma}\left(\frac{2z}{H} - 1\right)\right) \tag{50}$$

As in the $M < 1$ case, taking the limit as $\Gamma \to 0^+$ for the velocity field above recovers the same strictly radial, z-independent velocity field given in equation 11 and in mechanical dispersion studies that ignore buoyancy effects. This $M = 1$ velocity field is also consistent with the volumetric flux integral:

$$\phi\int_0^H\int_0^{2\pi} \frac{Q}{2\pi\phi HR}\left(1 - \sqrt{\Gamma}\left(\frac{2z}{H} - 1\right)\right)(Rd\theta dz) = Q \tag{51}$$

Using the same definition of $r_1(t)$ and $r_2(t)$ used previously, the $M = 1$ sharp interface solution and velocity field obtained in equation 50 yields:

$$r_1(t) = \sqrt{\frac{Q}{\pi\phi H}(1+\Gamma)t}\exp\left\{\alpha\sqrt{d}\left(\frac{Q}{\pi\phi H}(1+\Gamma)t\right)^{\frac{-1}{4}}\right\} \tag{52}$$

$$r_2(t) = \sqrt{\frac{Q}{\pi\phi H}(1+\Gamma)t} \tag{53}$$

Where the difference $r_1(t) - r_2(t)$ converges to zero as the dispersivity length $d \to 0^+$ as expected. Once more, nondimensionalizing the difference between the radial extent of the 1% concentration boundary (evaluating equation 28 with $A(Z)$ from equation 50) and the sharp interface solution in equation 49 at $z = 0$ gives the function for the $M = 1$ case:

$$R_1(T) - R_2(T) = \sqrt{(1+\Gamma)T}\left(\exp\left\{\alpha((1+\Gamma)T)^{\frac{-1}{4}}\right\} - 1\right) \tag{54}$$

Which is once more a strictly positive function for $T > 0$ and physical values of $0 < \Gamma < 1$. Having the same form of T dependence as the seperation functions for the $M < 1$ and $M > 1$ cases, the distance between the 1% concentration region and the would-be sharp interface initially decreases with time, before the 1% concentration boundary monotonically recedes from the sharp interface solution's position after a critical time. For $M = 1$, this occurs when:

$$T_{crit} = \frac{1}{1+\Gamma}\left(\frac{\alpha}{W_0\{-2e^{-2}\}+2}\right)^4 \tag{55}$$

For $\Gamma = 0.05$, $T_{crit} \approx 1.9$ for the $M = 1$ case. A plot of $R_1(T) - R_2(T)$ is given in figure 4 with a domain of $0 < \Gamma < 1$ and $T = 10, 100$ and 1000

D. A Carbon Capture and Storage Application

As a final demonstration of the concentration profile produced by mechanical dispersion, consider the following example with physical values. One of the motivations for the present paper is developing a novel CCS enhancement. The $M = 1$ case can be used to represent injecting aqueous carbon dioxide into an aquifer for CCS. Since the aqueous CO_2 solution being injected would be more dense than the resident brine, the original $M = 1$ sharp interface solution must first

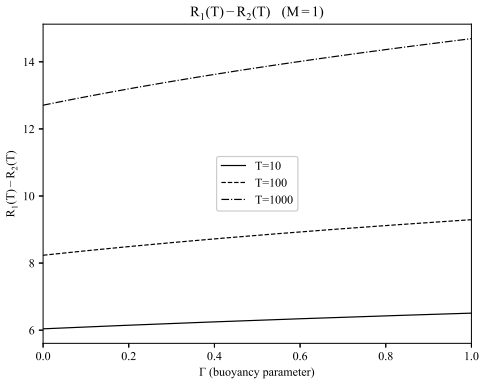

FIG. 4. The dimensionless difference between the 1% relative concentration boundary and the immiscible interface solution at the top of the aquifer ($M = 1$)

be reflected in the vertical direction (i.e. replacing $h(r,t)$ with $H - h(r,t)$) to reflect the fact that the injected solution will now sink below the resident brine, rather than rising above it[38].

In this aproach, instead of injecting pure CO_2, it is dissolved in brine produced from a target aquifer and reinjected back into the formation[39,40]. This problem's formulation becomes identical to injecting contaminant fluid in porous media, but the importance of dispersion is increased due to much larger scales of injection. While the injection of aqueous CO_2 into an aquifer has not yet been implemented in a large scale CCS project, the dissolving mechanisms and benefits over pure CO_2 injection (such as significantly reducing the risk of carbon leakage through the surface due to buoyancy) have been proposed in the engineering literature[41–43]. The CCS potential of such a project has also inspired empirical research on the geochemical effects of aqueous CO_2 flowing through porous rock[44].

Typical aquifer parameters and a typical CCS project injection rate and duration are given in table II, and figure 5 illustrates an example of these transition zone boundaries ($c/c_o = 0.99$ and $c/c_o = 0.01$) compared to the reflected $M = 1$ sharp interface given by Guo et al.[27].

It is clear from the plot in figure 5 that the concentration transition zone due to mechanical dispersion is considerably spread around the sharp interface solution's would-be location, with the 1% and 99% boundaries separated by several hundred metres. The radial extent of the interface and the boundaries (to the nearest metre) at the top and bottom of the aquifer are summarized in table III:

Using the application parameters from table II and the velocity field from equation 50, the mechanical dispersion term $d\|\boldsymbol{v}\|$ from the diffusivity tensor (equation 16) can be evaluated at certain positions in the aquifer. For example, using the two positions along the "sharp interface" given in table III (which lie between the 1% and 99% concentration cut offs), the dispersion term $d\|\boldsymbol{v}\| \approx 9.86 \times 10^{-6} m^2/s$ at $r = 1395m, z = 100m$, and $d\|\boldsymbol{v}\| \approx 1.94 \times 10^{-5} m^2/s$ at $r = 1112m, z = 0m$. In comparison, the coefficient of molecular diffusion for CO2 dissolved in water is about $1.92 \times 10^{-9} m^2/s$ [45], which is several orders of magnitude less than the above dispersion terms. Thus, neglecting the effects of molecular diffusion and using the simplified ADE in equation 17 is appropriate for this injection application.

As a final verification of this analysis, figure 6 contains a plot of the $M = 1$ sharp interface, 1% and 99% relative concentration boundaries with most of the same CCS parame-

TABLE II. List of CCS quantities used to plot sharp interface and transition zone/concentration boundaries.

Variable	Quantity [Dimensions]	Value
Q	Volume injection rate [L^3T^{-1}]	1,000,000 m^3/year
H	Aquifer height [L]	100 m
M	Viscosity ratio (res./inj. fluid)	1
Γ	Buoyancy parameter	0.05
ϕ	Aquifer Porosity	0.1
t	Time elapsed [T]	50 years
d	Dispersivity scale [L]	35 m

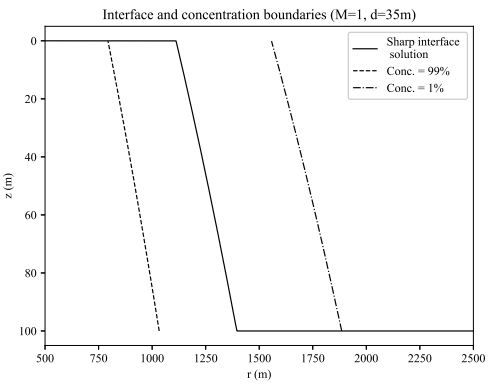

FIG. 5. The solution for the $M = 1$ sharp interface with the boundaries for 1% and 99% relative concentration of the injected fluid, using the CCS paramters in table II.

TABLE III. Example radial extents for the $M = 1$ Interface, 1% and 99% concentration boundaries at the top and bottom of the aquifer for the CCS example.

	99% boundary	Interface solution	1% boundary
At $z = 100$ m:	$r = 1034$ m	$r = 1395$ m	$r = 1885$ m
At $z = 0$ m:	$r = 794$ m	$r = 1112$ m	$r = 1558$ m

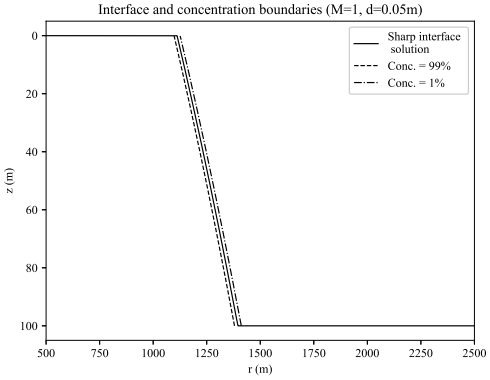

FIG. 6. The solution for the $M = 1$ sharp interface with the boundaries for 1% and 99% relative concentration of the injected fluid, using d=0.05m and the other CCS paramters in table II.

ters from table II, except the dispersivity scale length is set to $d = 0.05$m. The plot in figure 6 shows that these concentration boundaries nearly coincide with the sharp interface for all z values such that $0 \le z \le H$. Thus, in the limit of zero dispersion, the original sharp interface/saturated concentration profile is recovered from the smooth concentration profile derived above.

IV. DISCUSSION

It is clear that a mechanical dispersion model for an injection well can allow for an injected fluid concentration transition zone that is spread considerably on either side of a sharp interface solution. For the three examples used throughout section III, the 1% relative concentration boundary location was found to always lie radially ahead of, and increasingly recede from, the original interface solution over time. The significance of the derived "seperation" functions $R_1(T) - R_2(T)$ remaining strictly positive and increasing (after a relatively brief initial period) with respect to time is that detectable traces of the injected fluid appear increasingly further outward due to mechanical dispersion than otherwise predicted by a zero-dispersion sharp interface solution. These derived seperation functions are all well defined for all positive time values and their corresponding M and Γ values.

The three sharp interface cases examined were solutions from Guo et al.[27], where the viscosity differences between the injected fluid and resident fluid were the primary factor determining the interfaces' geometries. For all three cases, the dimensionless seperation between the 1% relative concentration boundary and the original sharp interface at the top of the aquifer $R_1(T) - R_2(T)$ is found to lie approximately in the range 6-13, with larger differences occuring at later dimensionless times T. This corresponds to 1% concentration traces of the injected fluid for a given interface geometry lying 6-13 dispersivity lengths ahead of the furthest radial extent of the sharp interface solution (which occurs at $z = 0$). For typical CCS injection paramters, this means the non-dispersion solution underestimates the radial extent of injectant traces of 1% relative concentration by several hundred meters.

Thus the results in section III illustrate the need to account for mechanical dispersion in the fluids' evolution in the aquifer for many practical injection cases. Note that the relative concentration c/c_o itself is a variable quantity, and the choice of using a 1% relative concentration boundary is not unique. The same procedure applied in section III may be used for smaller concentration cutoffs (< 1%) and will yield injectant traces even futher beyond a sharp interface solution than the derived seperations. Larger relative concentration cutoff values will have boundaries which lie closer to the sharp interface solution, and may lie behind it rather than beyond it (e.g. as seen with the 99% concentration boundary). The values 1% and 99% used in this analysis represent intuitive boundaries to enclose a region with a significant concentration gradient.

The location of the 1% relative concentration boundary considered in section III is particularly useful for injection well engineering applications. For example, if one wanted to know the extent of an injected contaminant's presence after a period of time, the sharp interface solution would tend to underestimate the upper limit of its radial position; as seen in figures 5 and 6, the interface solution lies within the concentration transition zone due to mechanical dispersion. In practice, if aquifer water were to be sampled from just outside the furthest extent of the sharp interface solution at a given height in the aquifer, it could still contain considerable traces (> 1%) of the injected contaminant. For safety measures, the 1% boundary location (or the boundary of a desired cutoff concentration, e.g. 5%, 0.1%, etc.) should be treated as a worst-case scenario for sampling uncontaminated water.

A physical example is given in section III D for the equal viscosity case, which can be applied to an aqueous carbon dioxide solution being injected for CCS. From the results summarized in table III, the 99% boundary is found to lie 257-419 m behind the sharp interface solution, and the 1% boundary is found to lie 413-531 m ahead of the sharp interface solution using the example values in table II. Comparing these physical results to the nondimensional ones for $M = 1$, the difference between the interface and the 1% boundary at $z = 0$ (413 m) is 11.8 times the dispersivity scale $d = 35$m after 50 years of injection (corresponding to a dimensionless duration of $T \approx 1300$); this is consistent with the 6-13 range for the dimensionless separation for a similar duration seen in figure 4.

V. CONCLUSIONS

The goal of this study was to outline a mathematical technique accounting for the effect of mechanical dispersion on the evolution of injection well fluids propagating in a con-

fined, porous aquifer. In the case of zero dispersion, a sharp interface is formed between the injected and resident fluids and evolves through the aquifer over time. The 2-D geometry of a sharp interface solution (which arises due to buoyancy and viscosity effects) is interpreted to "guide" the geometry of the fluids' velocity field within the aquifer.

Given an analytic expression for a sharp interface solution (presented in terms of its height $h(r,t)$), the time dependent radial velocity of the interface can be found by differentiating its radial position with respect to time. Rearranging the interface solution for time yields the "intersection time" when a specific aquifer position (r,z) is intersected by the propagating interface. Inserting this intersection time into the radial position time derivative yields a position dependent velocity field throughout the aquifer, of the incompressible form $\boldsymbol{v} = \frac{A(z)}{r}\hat{\boldsymbol{r}}$: the function $A(z)$ encodes the fluid characteristics underlying the original sharp interface solution. Substituting $A(z)$ into an analytic ADE solution gives the 2-D concentration profile of the fluids due to mechanical dispersion, with the vertically dependent effects (e.g. buoyancy) included.

One result of this technique of practical interest is to obtain the location of a "boundary" of a desired relative concentration of the injected substance. For real world applications involving contaminant injection into aquifers, such boundaries allow for defining a "cut off" position of arbitrarily low relative concentration, beyond which the groundwater may be considered uncontaminated. This will allow for engineers to plan injection well sites more cautiously for these applications and quantify "worst case scenarios" for contaminant presence away from the injection well.

It is worth mentioning that the choice of using the equation from Dagan[33] and its inversion for the concentration and radial extent of the cutoff boundaries is not unique. Approximate solutions for the ADE exist in other forms, such as that given by Tang and Babu[16]. The general nature of the transformation outlined in this study should in principle allow for any sharp interface and ADE solutions to be used to obtain a dispersive concentration profile throughout an aquifer.

ACKNOWLEDGMENTS

Financial support for this work provided by Natural Sciences and Engineering Research Council of Canada (NSERC). The authors have no conflicts to disclose.

[1] S. Buckley and M. Leverett, "Mechanism of fluid displacement in sands," Transactions of the AIME **146**, 107–116 (1942).
[2] B. Loret, *Fluid Injection in Deformable Geological Formations: Energy Related Issues* (Springer International Publishing, 2019).
[3] C. Browne, A. Shih, and S. Datta, "Pore-scale flow characterization of polymer solutions in microfluidic porous media," Small **16**, e1903944 (2020).
[4] H. Prommer and P. Stuyfzand, "Identification of temperature-dependent water quality changes during a deep well injection experiment in a pyritic aquifer," Environ. Sci. Technol. **39**, 2200–2209 (2005).
[5] J. Gibbons and H. Chalmers, "Carbon capture and storage," Energy Policy **36**, 4317–4322 (2008).
[6] A. Niemi, J. Bear, and J. Bensabat, *Geological Storage of CO2 in Deep Saline Formations* (Springer Netherlands, 2017).
[7] X. Dong and Z. Duan, "Co2 plume evolution in the saline aquifer under various injection operations for ccs," IOP Conf. Ser.: Earth Environ. Sci **585**, 12182 (2020).
[8] M. Swickrath, S. Mishra, and P. Ganesh, "An evaluation of sharp interface models for co2-brine displacement in aquifers," Groundwater **54**, 336–344 (2016).
[9] M. Abdelaal and M. Zeidouni, "Pressure falloff testing to characterize co2 plume and dry-out zone during co2 injection in saline aquifers," Int. J. Greenh. **103**, 103160 (2020).
[10] P. Ganesh and S. Mishra, "Simplified physics model of co2 plume extent in stratified aquifer-caprock systems," Greenhouse Gas Sci Technol. **6**, 70–82 (2016).
[11] J. Nordbotten, M. Celia, and S. Bachu, "Injection and storage of co2 in deep saline aquifers: Analytical solution for co2 plume evolution during injection," Transp. Porous Media **58**, 339–360 (2005).
[12] J. Nordbotten and M. Celia, "Similarity solutions for fluid injection into confined aquifers," J. Fluid Mech. **561**, 307–327 (2006).
[13] R. Juanes, C. MacMinn, and M. Szulczewski, "The footprint of the co2 plume during carbon dioxide storage in saline aquifers: Storage efficiency for capillary trapping at the basin scale," Transp. Porous Media **82**, 19–30 (2010).
[14] C. Fetter, *Applied hydrogeology: Fourth edition* (Prentice Hall, 2001).
[15] J. Hoopes and D. Harleman, "Dispersion in radial flow from a recharge well," J. Geophys. Res. **72**, 3595–3607 (1967).
[16] D. Tang and D. Babu, "Analytical solution of a velocity dependent dispersion problem," Water Resour. Res. **15**, 1471–1478 (1979).
[17] G. Hwang, "A unified approach to two-dimensional linear advection-dispersion equation in cylindrical coordinates on a finite domain," Int. J. Heat Mass Transf. **164**, 120569 (2021).
[18] C. Liang, S. Hsu, and J. Chen, "An analytical model for solute transport in an infiltration tracer test in soil with a shallow groundwater table," J. Hydrol. **540**, 129–141 (2016).
[19] A. Sanskrityayn, V. Singh, V. Bharati, and N. Kumar, "Analytical solution of two-dimensional advection–dispersion equation with spatio-temporal coefficients for point sources in an infinite medium using green's function method," Environ. Fluid. Mech. **18**, 739–757 (2018).
[20] E. du Toit, M. O'brien, and R. Vann, "Positivity-preserving scheme for two-dimensional advection–diffusion equations including mixed derivatives," Comput. Phys. Commun. **228**, 61–68 (2018).
[21] M. Singh, S. Rajput, and R. Singh, "Study of 2d contaminant transport with depth varying input source in a groundwater reservoir," Water Supply **21.4**, 1464–1480 (2021).
[22] Z. Ahmad, G. Ashraf, and A. Fryar, "Implications and concerns of deep-seated disposal of hydrocarbon exploration produced water using three-dimensional contaminant transport model in bhit area, dadu district of southern pakistan," Environ. Monit. Assess. **170**, 395–406 (2010).
[23] I. Jankovic and A. Fiori, "Analysis of the impact of injection mode in transport through strongly heterogeneous aquifers," Adv. Water Resour. **33**, 1199–1205 (2010).
[24] S. Comba and J. Braun, "An empirical model to predict the distribution of iron micro-particles around an injection well in a sandy aquifer," J. Contam. Hydrol. **132**, 1–11 (2012).
[25] A. Cahill, P. Marker, and R. Jakobsen, "Hydrogeochemical and mineralogical effects of sustained co2 contamination in a shallow sandy aquifer: A field-scalecontrolled release experiment," Water Resour. Res. **50**, 1735–1755 (2014).
[26] F. White, *Fluid mechanics: Seventh edition* (McGraw-Hill, 2011).
[27] B. Guo, Z. Zheng, M. Celia, and H. Stone, "Axisymmetric flows from fluid injection into a confined porous medium," Phys. Fluids **28**, 022107 (2016).
[28] H. Haitjema and M. Anderson, "Darcy velocity is not a velocity," Groundwater **54**, 1–1 (2015).
[29] T. Stocker, *Introduction to climate modelling* (Springer, 2011).
[30] J. Bear, "On the tensor form of dispersion in porous media," J. Geophys. Res. **66**, 1185–1197 (1961).
[31] S. Neuman, C. Winter, and C. Newman, "Stoachastic theory of field-scale fickian dipsersion in anistropic porous media," Water Resour. Res. **23**, 453–466 (1987).
[32] J. Pickens and G. Grisak, "Modeling of scale-dependent dispersion in hydrogeologic systems," Water Resour. Res. **17**, 1701–1711 (1981).
[33] G. Dagan, "Perturbation solutions of the dispersion equation in porous

mediums," Water Resour. Res. **7**, 135–142 (1971).
[34]P. Hsieh, "A new formula for the analytical solution of the radial dispersion problem," Water Resour. Res. **22**, 1597–1605 (1986).
[35]K. Lai, C. Liu, C. Liang, J. Chen, and B. Sie, "A novel method for analytically solving a radial advection-dispersion equation," J. Hydrol. **542**, 532–540 (2016).
[36]P. Hsieh and H. Yeh, "Semi-analytical and approximate solutions for contaminant transport from an injection well in a two-zone confined aquifer system," J. Hydrol. **519**, 1171–1176 (2014).
[37]C. Huang, C. Tong, W. Hu, H. Yeh, and T. Yang, "Analysis of radially convergent tracer test in a two-zone confined aquifer with vertical dispersion effect: Asymmetrical and symmetrical transports," J. Hazard. Mater. **377**, 8–16 (2019).
[38]S. Pegler, H. Huppert, and J. Neufeld, "Fluid injection into a confined porous layer," J. Fluid Mech. **745**, 592–620 (2014).
[39]F. Cao, D. Eskin, and Y. Leonenko, "Modeling of ex-situ dissolution for geologic sequestration of carbon dioxide in aquifers," J. Pet. Sci. Eng. **187**, 106835 (2020).
[40]F. Cao, D. Eskin, and Y. Leonenko, "Modeling of carbon dioxide dissolution in an injection well for geologic sequestration in aquifers," Energy **221**, 119780 (2021).
[41]S. Zendehboudi, A. Khan, S. Carlisle, and Y. Leonenko, "Ex situ dissolution of co2: A new engineering methodology based on mass-transfer perspective for enhancement of co2 sequestration," Energy Fuels **25**, 3323–3333 (2011).
[42]A. Vikhansky, D. Eskin, A. Budaraju, and Y. Leonenko, "Optimization of carbon dioxide dissolution in an injection tubing for geologic sequestration in aquifers," J. Pet. Sci. Eng. **208**, 109805 (2022).
[43]S. Shariatipour, E. Mackay, and G. Pickup, "An engineering solution for co2 injection in saline aquifers," Int. J. Greenh. **53**, 98–105 (2016).
[44]M. Voltolini and J. Ajo-Franklin, "The effect of co2-induced dissolution on flow properties in indiana limestone: An in situ synchrotron x-ray microtomography study," Int. J. Greenh. **82**, 38–47 (2019).
[45]E. Cussler, *Diffusion: Mass Transfer in Fluid Systems (3ed)* (Cambridge University Press, 2009).